Journal of Sound and Vibration (1999) **222**(1), 65–84
Article No. jsvi.1998.0065, available online at http://www.idealibrary.com on IDEAL

A SPACE–TIME FINITE ELEMENT METHOD FOR ELASTO-PLASTIC SHOCK DYNAMICS

R. P. S. HAN

Department of Mechanical Engineering, The University of Iowa, Iowa City, IA 52242, U.S.A.

AND

J. LU

Department of Mechanical Engineering, University of California, Berkeley, CA 94720, U.S.A.

(*Received* 19 *March* 1998, *and in final form* 16 *October* 1998)

A space–time finite element method (STFEM) for elastoplastic dynamic analysis is proposed in this paper. A weak form of the governing equation which corresponds to the conservation of impulse-momentum (the shock-momentum equation) is established, based on which STFEM equations are derived. A family of linear temporal shape functions is studied, which for linear elasticity, the ensuing STFEM algorithm is equivalent to the Newmark algorithm with $\gamma = 0{\cdot}5$. Rate-independent plasticity is incorporated into the model. As a numerical example, a cantilever beam under shock loading is analyzed. The results show that the propagation of shock waves is drastically slowed down by the presence of plasticity. Also, because the plastic deformation tends to be localized in the vicinity of the impact, a full transient analysis is essential, in order to accurately determine the locations of the plastic hinges.

1. INTRODUCTION

The dynamic behavior of structures with elastoplastic constitutive equations has attracted considerable interest in the past three decades or so. In this paper, attention is focused on shock-loaded structures, and to compute their elastoplastic response, an unconventional finite element technique based on a unified space–time discretization approach is employed. Analytical treatment of shock-loaded structures via say, the limit analysis is quite popular. However, the models used are relatively simple with the results obtained by assuming *a priori* the locations of the plastic hinges. A more accurate handling of this problem, particularly when dynamic plasticity is involved, is to carry out a full transient response calculation. This would enable the time-history for quantities of interest to be traced and thus, permits some intriguing features such as localization phenomena to be captured and monitored. The procedure is, however, numerical

0022–460X/99/160065 + 20 $30.00/0

rather than analytical, and in this regard, the finite element method is extremely popular. In fact, it is fair to say that computational elastoplasticity is now well-established, and many general purpose finite element programs are available. The Galerkin finite element approach for dynamic analysis is to employ finite elements to discretize the spatial domain and a finite difference scheme for the time domain (see for example, references [1, 2]). Plasticity is incorporated as a physical non-linearity. From a methodology point of view, the plasticity problem is formulated by adding to the equations of motion of a deformable body, a set of equations regarding the evolution of state variables. The treatment of the rate form equations, notably by numerical integration, is now well known [3–6].

As mentioned, most finite element procedures for solving time dependent problems are based on a two-stage discretization: finite elements are employed first to reduce the partial differential equations into a system of ordinary differential equations in time, and then a finite difference technique is employed to perform the time-integration. This method is well understood and very popular. However, for problems involving rapid gradient changes, it may experience numerical difficulties. An alternative approach for dealing with transient dynamics that has attracted renewed interest in recent years, is to discretize both the space and time domains simultaneously. This concept of the space–time finite element method (STFEM) first emerged towards the late sixties [7–10]. The approach possesses a number of merits over the conventional finite element technique. As shown by Zienkiewicz [11] and subsequently by Tang *et al.* [12], STFEM is able to replicate a wide range of time integration schemes, particularly, the commonly used ones. With the introduction of discontinuous temporal finite elements [13–15], novel integration schemes which lead to stable and accurate results can be derived. An interesting application to a non-linear problem was demonstrated by Cella *et al.* [16]. Although numerical properties of the ensuing algorithm for handling nonlinear analysis are problem-dependent, generally, there are no guarantees of uniqueness and stability of the solutions, this procedure did show success in a number of cases.

STFEM for dynamic problem can also be derived from Hamilton's Law of Varying Action (or simply, Hamilton's Law), or equivalently, from a virtual work principle in both the space and time domains. Note that we are not referring to Hamilton's principle which is a special case of Hamilton's Law. In the former, the final and initial co-ordinates, and time must be known. A more in-depth discussion is presented in Bailey [17], and Baruch and Riff [18]. The STFEM equations formulated this way possess a clear physical meaning in that they relate the change of system momenta between two time-steps with the impulse arising from external and internal forces during the time interval considered. Thus, the resulting set of STFEM equations can be interpreted as the general law of impulse and momentum. This approach has been adopted here in our STFEM formulation. A weak form of the governing equations is derived from the virtual work principle. The advantage of using the weak form approach is that it can be physically interpreted as the generalized *law of conservation of impulse-momentum* and therefore, can be applied to a wider class of problems. Further details can be found in reference [19]. For simplicity, the

time discretization will be confined to a family of linear interpolations, and it can be shown that for linear elasticity, this algorithm is equivalent to the Newmark method with $\gamma = 0{\cdot}5$. Also, in the absence of physical damping in the system, the algorithm will not suffer from numerical damping. Incorporation of plasticity is achieved by assuming a temporal pattern of plastic flow during the time interval considered. In this way, the STFEM equations can be written explicitly. The model will be restricted to rate-independent plasticity only since implementation of the rate-dependent plasticity can be treated in a similar way.

2. A WEAK FORM OF THE GOVERNING EQUATIONS

2.1. GOVERNING EQUATIONS OF ELASTO-PLASTIC DYNAMIC PROBLEM

The dynamic problem of an elastoplastic body, assuming infinitesimal strains, is generally described by the following set of equations.

Equilibrium equation:

$$\mathbf{L}(\mathbf{s}) + \mathbf{f} = \boldsymbol{r}\ddot{\mathbf{u}} + \boldsymbol{c}\dot{\mathbf{u}} \quad \text{on} \quad \Omega \times I. \tag{1}$$

Strain-displacement relationship:

$$\mathbf{e} = \mathbf{L}_1(\mathbf{u}). \tag{2}$$

Constitutive relationship:

$$\dot{\mathbf{s}} = \mathbf{D}^{ep}\dot{\mathbf{e}}. \tag{3}$$

Boundary conditions:

$$\begin{aligned} &\mathbf{u}(\mathbf{x}, t) = \tilde{\mathbf{u}}(\mathbf{x}, t) \qquad \text{on } \partial\Omega_{\mathrm{u}} \times I, \\ &\mathbf{t}(\mathbf{x}, t) \equiv \mathbf{s}{\cdot}\mathbf{n} = \tilde{\mathbf{t}}(\mathbf{x}, t) \quad \text{on} \quad \partial\Omega_{\mathrm{s}} \times I. \end{aligned} \tag{4}$$

Initial conditions:

$$\mathbf{u}(\mathbf{x}, 0) = \mathbf{u}_0(\mathbf{x}), \qquad \dot{\mathbf{u}}(\mathbf{x}, 0) = \dot{\mathbf{u}}_0(\mathbf{x}). \tag{5}$$

Note that Ω is the region the body occupies; $I =]0, T[$ is the time domain; $\mathbf{s}, \mathbf{e}, \mathbf{u}$ are the generalized stress (or stress resultant), strain and displacement vectors; $\mathbf{L}$, $\mathbf{L}_1$ denote differential operators in the spatial domain, the meaning of which depend on the specific problem; a dot denotes time derivative; $\boldsymbol{r}$, $\boldsymbol{c}$ are the inertial and viscous damping matrices, positive or semi-positive definite; $\mathbf{f}$ is the external force vector; $\partial\Omega_u$ and $\partial\Omega_s$ denote the exclusive parts of the boundaries on which the displacement $\mathbf{u}$ and traction force $\mathbf{t}$ are prescribed; and $\mathbf{n}$ is the outward normal vector on $\partial\Omega_{\mathrm{s}}$. For the sake of simplicity, it will be assumed that $\tilde{\mathbf{t}}(\mathbf{x}, t) = 0$ in the remainder of the paper. At this point, plasticity is simply characterized as a rate-form constitutive relation between stress and strain, with a more detailed description to be introduced in succeeding sections. Note that for work hardening materials, equations (1)–(5) specify a well-posed initial-boundary value problem, from which a unique and stable incremental solution can be obtained.

2.2. A WEAK FORM OF GOVERNING EQUATIONS

The governing equations can be recasted into a weak form as follows. Find

$$\mathbf{u} : \mathbf{L}^*(\mathbf{u}) \in L^2(\Omega), \mathbf{u}|_{\partial\Omega_u} = \tilde{\mathbf{u}}(\mathbf{x}, t),\ \delta\mathbf{u}|_{\partial\Omega_u} = 0,$$

such that

$$\int_I (\boldsymbol{r}\ddot{\mathbf{u}}, \delta\mathbf{u})_\Omega \,\mathrm{d}t - \int_I (\mathbf{s}, \mathbf{L}^*(\delta\mathbf{u}))_\Omega \,\mathrm{d}t - \int_I (\boldsymbol{c}\dot{\mathbf{u}}, \delta\mathbf{u})_\Omega \,\mathrm{d}t + \int_I (\mathbf{f}, \delta\mathbf{u})_\Omega \,\mathrm{d}t = (\boldsymbol{r}\dot{\mathbf{u}}, \delta\mathbf{u})_\Omega \Big|_{t_1}^{t_2} \quad (6)$$

in which $(\mathbf{a}, \mathbf{b})_\Omega = \int_\Omega \mathbf{a} \cdot \mathbf{b} \,\mathrm{d}\Omega$; $\mathbf{L}^*$ denotes the adjoint operator of $\mathbf{L}$ defined by the bilinear form $(\cdot,\cdot)_\Omega$; $I =]t_1, t_2[$; and $L^2(\Omega)$ denotes the space of square-integrable functions defined on Ω. A straight forward manipulation shows that the Euler–Lagrange equation of the above functional yields the equilibrium equation (1) and the prescribed traction boundary conditions (4). Furthermore, the velocity can be treated as an independent variable. To this end, we will introduce a new variable $\mathbf{v}$ such that

$$\mathbf{v} - \dot{\mathbf{u}} = 0, \quad (7)$$

where $\mathbf{v}: \mathbf{v} \in L^2(\Omega),\ \mathbf{v}|_{\partial\Omega_u} = \dot{\tilde{\mathbf{u}}}(\mathbf{x}, t),\ \delta\mathbf{v}|_{\partial\Omega_u} = 0$. Adding a least square term to equation (6) yields

$$\int_I (\boldsymbol{r}\ddot{\mathbf{u}}, \delta\mathbf{u})_\Omega \,\mathrm{d}t - \int_I (\mathbf{s}, \mathbf{L}^*(\delta\mathbf{u}))_\Omega \,\mathrm{d}t - \int_I (\boldsymbol{c}\dot{\mathbf{u}}, \delta\mathbf{u})_\Omega \,\mathrm{d}t$$

$$+ \int_I (\mathbf{f}, \delta\mathbf{u})_\Omega \,\mathrm{d}t - \int_I (\boldsymbol{r}(\dot{\mathbf{u}} - \mathbf{v}), \delta\dot{\mathbf{u}} - \delta\mathbf{v})_\Omega \,\mathrm{d}t = (\boldsymbol{r}\dot{\mathbf{u}}, \delta\mathbf{u})_\Omega \Big|_{t_1}^{t_2}, \quad (8)$$

which after integration and performing some algebraic manipulations leads to

$$\int_I (\boldsymbol{r}\mathbf{v}, \delta\dot{\mathbf{u}})_\Omega \,\mathrm{d}t - \int_I (\mathbf{s}, \mathbf{L}^*(\delta\mathbf{u}))_\Omega \,\mathrm{d}t - \int_I (\boldsymbol{c}\dot{\mathbf{u}}, \delta\mathbf{u})_\Omega \,\mathrm{d}t$$

$$+ \int_I (\mathbf{f}, \delta\mathbf{u})_\Omega \,\mathrm{d}t = (\boldsymbol{r}\dot{\mathbf{u}}, \delta\mathbf{u})_\Omega \Big|_{t_1}^{t_2} \int_I (\boldsymbol{r}(\mathbf{v} - \dot{\mathbf{u}}), \delta\mathbf{v})_\Omega \,\mathrm{d}t = 0. \quad (9)$$

Observe that one now has the variational equation of the Hellinger–Reissner principle [6] for dynamic problems. The physical meaning of equation (6) is obvious: it can be regarded as the weak form of the law of impulse-momentum which states that the change of the system momenta during any two time steps is equal to the impulse from the external and internal forces acting on that system. Perhaps it would be more appropriate to call it the shock-momentum equation. Equation (9) represents its counterpart in which the displacement and velocity are regarded as independent variables. Note that the initial value enters through the time-limit terms (right-hand side of equation (9)) This implies that its solution can be constructed in a step-by-step manner.

3. STFEM FORMULATION

3.1. STFEM DISCRETIZATION

The finite element discretization of equation (9) will now be formulated. A space–time finite element is constructed as a union of the conventional finite element and an appropriately chosen time discretization scheme. That is, for a conventional finite element partitioning

$$\tilde{\Omega} = \bigcup_{e=1}^{nelem} \Omega_e, \tag{10}$$

and a partitioning in time

$$I \equiv]0, T[= \bigcup_{n=1}^{N} I_n,\ I_n =]t_n, t_{n+1}[\,, \tag{11}$$

the space–time finite element is defined as

$$Q_e = \Omega_e \times I_n. \tag{12}$$

The finite element representation of equation (9) then reads, find the solutions over the discretized domain $\mathbf{u}^k$, $\mathbf{v}^h$

$$\begin{aligned} \mathbf{u}^h &\in \mathbf{U}^h = \{\mathbf{u}^h : \mathbf{L}(\mathbf{u}^h) \in L^2(\cup Q^e), \mathbf{u}^h|_{\partial\Omega} = \tilde{\mathbf{u}}(\mathbf{x}, t)\}, \\ \mathbf{v}^h &\in \mathbf{V}^h = \{\mathbf{v}^h : \mathbf{L}(\mathbf{v}^h) \in L^2(\cup Q^e), \mathbf{v}^h|_{\partial\Omega} = \dot{\tilde{\mathbf{u}}}(\mathbf{x}, t)\}, \end{aligned} \tag{13}$$

such that

$$\int_I (\boldsymbol{r}\mathbf{v}^h, \delta\dot{\mathbf{u}}^h)_\Omega \,\mathrm{d}t - \int_I (\mathbf{s}^h, \mathbf{L}^*(\delta\mathbf{u}^h))_\Omega \,\mathrm{d}t - \int_I (\boldsymbol{c}\dot{\mathbf{u}}^h, \delta\mathbf{u}^h)_\Omega \,\mathrm{d}t + \int_I (\mathbf{f}, \delta\mathbf{u}^h)_\Omega \,\mathrm{d}t = (\boldsymbol{r}\dot{\mathbf{u}}^h, \delta\mathbf{u}^h)_\Omega \Big|_{t_1}^{t_2},$$

$$\int_I (\boldsymbol{r}(\mathbf{v}^h - \dot{\mathbf{u}}^h), \delta\mathbf{v}^h)_{\Omega_e} \,\mathrm{d}t = 0 \text{ for every } \Omega_e, \tag{14}$$

on any time interval I.

3.2. TEMPORAL INTERPOLATIONS

Our attention will be confined to a particular family of piecewise linear time interpolations. That is, for a time-slab $t \in I_n =]t_n,\ t_{n+1}[$; $\Delta t = t_{n+1} - t_n$. The displacement and velocity can be approximated as

$$\mathbf{u}^h(t) = N_n(t)\mathbf{u}_n^h(\mathbf{x}) + N_{n+1}(t)\mathbf{u}_{n+1}^h(\mathbf{x}), \quad \mathbf{v}^h(t) = (1 - \xi)\mathbf{v}_n^h(\mathbf{x}) + \xi\mathbf{v}_{n+1}^h(\mathbf{x}), \tag{15}$$

where $\xi = t - t_n/\Delta t$ and $u_n^h, \mathbf{v}_n^h$ are the nodal values. The following requirements for the temporal shape function N_n have to be satisfied:

$$N_i(t_j) = \delta_{ij}, N_n(t) + N_{n+1}(t) = 1, \int_{I_n} N_n(\tau)\,\mathrm{d}\tau = \frac{\Delta t}{2}, \int_{I_n} N_{n+1}(\tau)\,\mathrm{d}\tau = \frac{\Delta t}{2}, \tag{16}$$

and if

$$\int_{I_n} N_n(\tau)N_{n+1}(\tau)\,\mathrm{d}\tau = \beta\Delta t, \tag{17}$$

where β is a constant, one has

$$\int_{I_n} (N_n(\tau))^2\,\mathrm{d}\tau = \left(\frac{1}{2}-\beta\right)\Delta t, \quad \int_{I_n} (N_{n+1}(\tau))^2\,\mathrm{d}\tau = \left(\frac{1}{2}-\beta\right)\Delta t. \tag{18}$$

With these considerations, and possibly further time-interpolations for stress, the temporal integration of equation (14) can be carried out. For clarity, spatial interpolations will be discussed in the following subsection and then provide the explicit STFEM equations.

3.3. SPATIAL INTERPOLATIONS AND STFEM EQUATIONS

As is customary in a finite element formulation, the spatial discretization is performed as

$$\mathbf{u}_i^h(\mathbf{x}) = \mathbf{N}\mathbf{U}_i, \quad \mathbf{v}_i^h(\mathbf{x}) = \mathbf{N}\mathbf{V}_i, \quad i = 1, \ldots N, \tag{19}$$

in which $\mathbf{N}$ denotes the spatial shape functions and $\mathbf{U}_i$, $\mathbf{V}_i$ the nodal values at a certain time-step. The general strain vector $\mathbf{e}$ is then given by

$$\mathbf{e} = \mathbf{B}\mathbf{U}, \tag{20}$$

where

$$\mathbf{B} = \mathbf{L}_1(\mathbf{N}(\mathbf{x})). \tag{21}$$

Note that the specific form of the differential operator in the spatial domain $\mathbf{L}_1$ is dependent on the problem being investigated. The following matrices and vectors can be subsequently obtained:

$$\mathbf{M} = (\mathbf{N}, \boldsymbol{r}\boldsymbol{N})_\Omega, \quad \mathbf{C} = (\mathbf{N}, \boldsymbol{c}\mathbf{N})_\Omega, \quad \mathbf{F} = (\mathbf{N}, \mathbf{f})_\Omega, \quad \mathbf{P} = (\mathbf{B}, \mathbf{s})_\Omega, \tag{22}$$

where $\mathbf{M}$, $\mathbf{C}$ are the mass and damping matrices, and $\mathbf{F}$, $\mathbf{P}$ the external and internal force vectors. Substituting the quantities in equations (22) into equation (14), after performing some algebraic operations, the following two sets of equations are derived:

$$\begin{aligned}
-\frac{\mathbf{M}}{2}(\mathbf{V}_{n+1}+\mathbf{V}_n) + \frac{\mathbf{C}}{2}(\mathbf{U}_{n+1}-\mathbf{U}_n) + \int_{I_n} N_n^T(\tau)\mathbf{P}\,\mathrm{d}\tau &= \mathbf{M}\dot{\mathbf{U}}_n + \int_{I_n} N_1^T(\tau)\mathbf{F}\,\mathrm{d}\tau,\\
-\frac{\mathbf{M}}{2}(\mathbf{V}_{n+1}+\mathbf{V}_n) - \frac{\mathbf{C}}{2}(\mathbf{U}_{n+1}-\mathbf{U}_n) - \int_{I_n} N_{n+1}^T(\tau)\mathbf{P}\,\mathrm{d}\tau &= \mathbf{M}\dot{\mathbf{U}}_{n+1} - \int_{I_n} N_2^T(\tau)\mathbf{F}\,\mathrm{d}\tau,
\end{aligned} \tag{23}$$

and

$$\left(\frac{1}{3}\mathbf{V}_{n+1}+\frac{1}{6}\mathbf{V}_n\right)\Delta t-\frac{1}{2}(\mathbf{U}_{n+1}-\mathbf{U}_n)=0,\ \left(\frac{1}{6}\mathbf{V}_{n+1}+\frac{1}{3}\mathbf{V}_n\right)\Delta t-\frac{1}{2}(\mathbf{U}_{n+1}-\mathbf{U}_n)=0. \tag{24}$$

Upon eliminating $\mathbf{V}_{n+1}, \mathbf{V}_n$ produces

$$\mathbf{M}\frac{\mathbf{U}_{n+1}-\mathbf{U}_n}{\Delta t}+\frac{\mathbf{C}}{2}(\mathbf{U}_{n+1}-\mathbf{U}_n)+\int_{I_n} N_n^T(\tau)\mathbf{P}\,\mathrm{d}\tau=\mathbf{M}\dot{\mathbf{U}}_n+\int_{I_n} N_n^T(\tau)\mathbf{F}\,\mathrm{d}\tau, \tag{25}$$

$$\mathbf{M}\frac{\mathbf{U}_{n+1}-\mathbf{U}_n}{\Delta t}+\frac{\mathbf{C}}{2}(\mathbf{U}_{n+1}-\mathbf{U}_n)-\int_{I_n} N_{n+1}^T(\tau)\mathbf{P}\,\mathrm{d}\tau=\mathbf{M}\dot{\mathbf{U}}_{n+1}-\int_{I_n} N_{n+1}^T(\tau)\mathbf{F}\,\mathrm{d}\tau. \tag{26}$$

The following equation follows immediately from equations (25) and (26):

$$\mathbf{M}(\dot{\mathbf{U}}_{n+1}-\dot{\mathbf{U}}_n)=\int_{I_n}\mathbf{F}\,\mathrm{d}\tau-\int_{I_n}\mathbf{P}\,\mathrm{d}\tau-\mathbf{C}(\mathbf{U}_{n+1}-\mathbf{U}_n), \tag{27}$$

which clearly states that the change of momentum of a system equals the impulse of the external, internal and damping forces. Equations (25) and (27) (or alternatively, equations (25) and (26)) constitute the STFEM equations for response computations. The response of the system can now be computed in a step-by-step manner. Initially, the unknown displacement $\mathbf{U}_{n+1}$ is calculated from equation (25) and then, the unknown velocity $\dot{\mathbf{U}}_{n+1}$ is calculated from equation (27) (or alternatively, from equation (26)). If plasticity is considered, then $\mathbf{P}$ is in general a non-linear function of, among others, $\mathbf{U}_{n+1}$, the solution of which can be achieved via Newton–Raphson iterations.

Remark 1

If a temporal interpolation was chosen for the internal force $\mathbf{P}$: $\mathbf{P}(t)=\mathbf{P}_n N_n(t)+\mathbf{P}_{n+1}N_{n+1}(t)$, as is the case of linear elastodynamics, *and* in the absence of damping, equations (25) and (26) are equivalent to the Newmark method with $\gamma=0{\cdot}5$, with the parameter β possessing the same meaning.

Remark 2

Remark 1 gives the connotation that the current approach is equivalent to the well-established Newmark method, at least for the case mentioned here. In fact, this proposed approach is much more versatile. For example, β for each element can be different, resulting in mixed integration schemes. In other words, the algorithm depicted by equations (25) and (26) is just a special case emanating from equation (14).

4. INCORPORATION OF RATE-INDEPENDENT PLASTICITY

In this section, the incorporation of plasticity into the STFEM model derived previously is discussed. Only rate-independent plasticity will be considered. It

provides a well-posed initial-boundary value problem for work hardening materials and guarantees a unique and stable incremental solution.

4.1. RATE-INDEPENDENT PLASTICITY

The constitutive equations governing elastoplastic deformations assuming infinitesimal strains, the associative flow rule and the associative hardening rule may be expressed in the form

$$\mathbf{e} = \mathbf{e}^e + \mathbf{e}^p, \quad \mathbf{s} = \mathbf{D}(\mathbf{e} - \mathbf{e}^p), \quad \dot{\mathbf{e}}^p = \dot{\lambda}\frac{\partial \phi(\mathbf{s}, \mathbf{q})}{\partial \mathbf{s}}, \quad \dot{\mathbf{q}} = -\dot{\lambda}\mathbf{H}\frac{\partial \phi(\mathbf{s}, \mathbf{q})}{\partial \mathbf{s}}, \tag{28}$$

where $\mathbf{e}^p$ is plastic strain, $\mathbf{q}$ is a set of plastic variables, $\dot{\lambda}$ is the plastic multiplier, $\mathbf{H}$ is the matrix of plastic moduli, and ϕ is the yield function such that any admissible state would have to satisfy

$$\phi(\mathbf{s}, \mathbf{q}) \leqslant 0. \tag{29}$$

The loading and unloading process is governed by the Kuhn–Tucker condition

$$\phi(\mathbf{s}, \mathbf{q}) \leqslant 0, \quad \dot{\lambda} \geqslant 0, \quad \dot{\lambda}\phi(\mathbf{s}, \mathbf{q}) = 0, \tag{30}$$

along with the consistency condition

$$\dot{\lambda}\dot{\phi}(\mathbf{s}, \mathbf{q}) = 0. \tag{31}$$

4.2. DISCRETIZATION SCHEME

The rate-form equations are then discretized to yield the constitutive relations suitable for the STFEM formulation. Assuming that the state variables at time t_n, i.e., $\mathbf{s}_n$, $\mathbf{e}_n$, $\mathbf{e}^p_n$, $\mathbf{q}_n$ are known, then $\mathbf{e}^p_{n+1}$, $\mathbf{q}_{n+1}$ can be predicted by the backward difference formulas

$$\mathbf{e}^p_{n+1} - \mathbf{e}^p_n = \dot{\lambda}\Delta t\frac{\partial \phi_{n+1}}{\partial \mathbf{s}_{n+1}} = \lambda_{n+1}\frac{\partial \phi_{n+1}}{\partial \mathbf{s}_{n+1}}, \tag{32}$$

$$\mathbf{q}^p_{n+1} - \mathbf{q}_n = -\dot{\lambda}\Delta t\mathbf{H}\frac{\partial \phi_{n+1}}{\partial \mathbf{q}_{n+1}} = -\lambda_{n+1}\mathbf{H}\frac{\partial \phi_{n+1}}{\partial \mathbf{q}_{n+1}}. \tag{33}$$

Also, the consistency condition is enforced at each time-step:

$$\dot{\lambda}\phi(\mathbf{s}_{n+1}, \mathbf{q}_{n+1}) = 0. \tag{34}$$

In view of the displacement interpolations in equation (15) and the strain–displacement relationship in equation (20), one has, for $t \in I_n$,

$$\mathbf{e}(t) = N_n(t)\mathbf{e}_n + N_{n+1}(t)\mathbf{e}_{n+1} = \mathbf{e}_n + N_{n+1}(t)(\mathbf{e}_{n+1} - \mathbf{e}_n), \tag{35}$$

and also

$$\mathbf{e}^p(t) = N_n(t)\mathbf{e}^p_n + N_{n+1}(t)\mathbf{e}^p_{n+1} = \mathbf{e}^p_n + N_{n+1}(t)(\mathbf{e}^p_{n+1} - \mathbf{e}^p_n). \tag{36}$$

It follows from equations (28), (32), (35) and (36) that

$$\mathbf{s}(t) = \mathbf{s}_n + \mathbf{D}\left(\mathbf{e}_{n+1} - \mathbf{e}_n - \lambda_{n+1}\frac{\partial \phi_{n+1}}{\partial \mathbf{s}_{n+1}}\right) N_{n+1}, \tag{37}$$

where $\mathbf{s}_n = \mathbf{D}(\mathbf{e}_n - \mathbf{e}_n^p)$. Substituting equation (37) into equation (25), and taking equations (16) and (17) into consideration, one obtains

$$\left(\frac{\mathbf{M}}{\Delta t^2} + \frac{\mathbf{C}}{2\Delta t}\right)(\mathbf{U}_{n+1} - \mathbf{U}_n) + \beta \mathbf{G}_{n+1} = \frac{1}{\Delta t}\left(\mathbf{M}\dot{\mathbf{U}}_n + \int_{I_n} N_n^T(\tau)\mathbf{F}\,\mathrm{d}\tau\right) - \frac{1}{2}\mathbf{P}_n, \tag{38}$$

in which the generalized internal force increment $\mathbf{G}_{n+1}$ is defined by

$$\mathbf{G}_{n+1} = \int_\Omega \mathbf{B}^T\mathbf{D}\left[\mathbf{B}(\mathbf{U}_{n+1} - \mathbf{U}_n) - \lambda_{n+1}\frac{\partial \phi_{n+1}}{\partial \mathbf{s}_{n+1}}\right] \mathrm{d}\Omega. \tag{39}$$

4.3. SOLUTION PROCEDURE

The full transient response can now be solved progressively. At each time-step, equation (38) is solved first to yield displacement $\mathbf{U}_{n+1}$, then equation (27) is employed to compute velocity $\dot{\mathbf{U}}_{n+1}$. Due to the plastic constitutive law, the former is non-linear. The following global–local iteration scheme is employed: a global equilibrium iteration is performed to provide a displacement increment, this increment is then inputted as a prescribed displacement to calculate λ_{n+1} via the enforcement of the discrete consistency condition. The objective, therefore, is to find $\mathbf{U}_{n+1}$ and λ_{n+1} such that

$$\begin{aligned} \mathbf{R}_{n+1} \equiv& \left(\frac{\mathbf{M}}{\Delta t^2} + \frac{\mathbf{C}}{2\Delta t}\right)(\mathbf{U}_{n+1} - \mathbf{U}_n) + \beta \mathbf{G}_{n+1} \\ &+ \frac{1}{2}\mathbf{P}_n - \frac{1}{\Delta t}\left(\mathbf{M}\dot{\mathbf{U}}_n + \int_{I_n} N_n^T(\tau)\mathbf{F}\,\mathrm{d}\tau\right) = 0, \\ \psi_{n+1} \equiv& \dot{\lambda}\phi(\mathbf{s}_{n+1},\ \mathbf{q}_{n+1}) = 0, \end{aligned} \tag{40}$$

are satisfied. To perform the global equilibrium iterations, the Newton–Raphson method is used. The procedure is described as follows, with particular emphasis on the dynamic tangential stiffness matrix $\mathbf{K}_T^i$. Using superscript i to indicate the iteration number, and given that $\mathbf{U}_{n+1}^0 = \mathbf{U}_n$, the iteration procedure can be expressed as,

$$\mathbf{K}_T^i\,\Delta\mathbf{U}_{n+1}^i = -\mathbf{R}_{n+1}^i, \quad \mathbf{U}_{n+1}^{i+1} = \mathbf{U}_{n+1}^i + \Delta\mathbf{U}_{n+1}^i. \tag{41}$$

Convergence is attained when the displacement increment attains

$$|\mathbf{R}_{n+1}^i|/|\mathbf{R}_{n+1}^0| \leqslant tol, \tag{42}$$

where *tol* is an assigned error tolerance. The dynamic tangent stiffness matrix $\mathbf{K}_T^i$ is given by

$$\mathbf{K}_T^i = \frac{\mathbf{M}}{\Delta t^2} + \frac{\mathbf{C}}{2\Delta t} + \beta \frac{\partial \mathbf{G}_{n+1}^i}{\partial \mathbf{U}_{n+1}^i}, \tag{43}$$

where the last term can be derived from the constitutive relation and the consistency condition. Note that β has the same meaning as that employed in the Newmark method. A particularly interesting result which is algorithmically consistent with the implicit backward Euler difference algorithm of Simo and Taylor [20] for yielding function satisfying $\partial^2\psi/(\partial \mathbf{s}\,\partial \mathbf{q}) = 0$ is derived as

$$\frac{\partial \mathbf{G}_{n+1}^i}{\partial \mathbf{U}_{n+1}^i} = \int_\Omega \mathbf{B}^T \left(\tilde{\mathbf{D}} - \frac{1}{h^i + a^i} \tilde{\mathbf{D}} \frac{\partial \phi_{n+1}}{\partial \mathbf{s}_{n+1}} \frac{\partial \phi_{n+1}}{\partial \mathbf{s}_{n+1}}^T \tilde{\mathbf{D}} \right) \mathbf{B}\, \mathrm{d}\Omega, \tag{44}$$

in which

$$\begin{aligned}
\tilde{\mathbf{D}} &= \left(\mathbf{D}^{-1} + \lambda_{n+1}^i \frac{\partial^2 \phi_{n+1}^i}{\partial \mathbf{s}_{n+1}^i\, \partial \mathbf{s}_{n+1}^i} \right)^{-1}, \\
a^i &= \frac{\partial \phi_{n+1}^i}{\partial \mathbf{s}_{n+1}^i}^T \left(\mathbf{D}^{-1} + \lambda_{n+1}^i \frac{\partial^2 \phi_{n+1}^i}{\partial \mathbf{s}_{n+1}^i\, \partial \mathbf{s}_{n+1}^i} \right)^{-1} \frac{\partial \phi_{n+1}^i}{\partial \mathbf{s}_{n+1}^i}, \\
h^i &= \frac{\partial \phi_{n+1}^i}{\partial \mathbf{q}_{n+1}^i}^T \left(\mathbf{H}^{-1} + \lambda_{n+1}^i \frac{\partial^2 \phi_{n+1}^i}{\partial \mathbf{q}_{n+1}^i\, \partial \mathbf{q}_{n+1}^i} \right)^{-1} \frac{\partial \phi_{n+1}^i}{\partial \mathbf{q}_{n+1}^i}.
\end{aligned} \tag{45}$$

The local iterations of enforcing the consistency condition known as *return mapping* has been extensively discussed elsewhere, see for example, reference [21].

5. APPLICATION TO A TIMOSHENKO BEAM

To demonstrate the method developed here, the elastoplastic response of a Timoshenko beam subjected to an impact load will be considered. The Timoshenko beam theory is chosen, in lieu of the simpler Euler–Bernoulli beam theory since the former not only models a wider range of beam types, but also, yields more accurate results, especially at higher vibration frequencies. The classical Timoshenko beam theory will first be re-formulated and a plasticity model incorporated into it. Then, a numerical example involving a cantilevered beam discretized by 20 elements and subjected to a tip impact load will be provided.

5.1. TIMOSHENKO BEAM THEORY

Assuming elastic constitutive behavior, the equations governing the free vibration of a Timoshenko beam depicted in Figure 1 can be written as,

$$\frac{\partial M}{\partial x} - Q = \rho I \frac{\partial^2 \psi}{\partial t^2}, \quad -\frac{\partial Q}{\partial x} = \rho A \frac{\partial^2 w}{\partial t^2}, \tag{46}$$

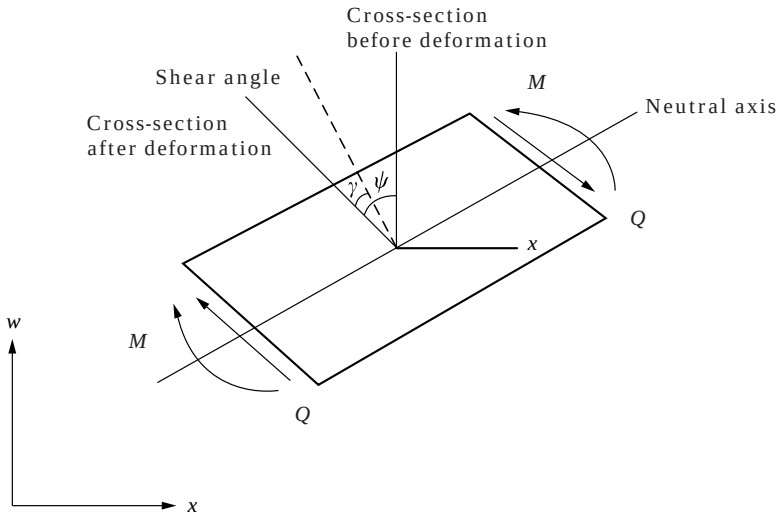

Figure 1. Timoshenko beam model, sign conventions and notations.

$$\kappa = \frac{\partial \psi}{\partial x}, \quad \gamma = \psi - \frac{\partial v}{\partial x}, \tag{47}$$

$$M = EI\kappa, \quad Q = GA\gamma, \tag{48}$$

where M is the bending moment and Q is the shear force, κ is the curvature of neutral axis, γ is the shear angle, w is the transverse displacement, ψ the rotating angle of the cross-section originally perpendicular to the neutral axis, and ρ, E, G, I, A are the usual material-cross sectional constants.

Employing the vector notations

$$\mathbf{u} = (\psi, w)^T, \quad \mathbf{e} = (\kappa, \gamma)^T, \quad \mathbf{s} = (M, Q)^T, \tag{49}$$

the form of the operators $\mathbf{L}$, $\mathbf{L}_1$ as well as matrices $\mathbf{D}$, $\mathbf{r}$ become evident. Due to its simplicity, the C^0 element of Hughes and Taylor [22] is used for spatial discretization. To overcome shear locking in this element a reduced integration is applied to its shear stiffness term.

5.2. PLASTICITY MODEL

The plasticity model employed for the analysis is now described, the details of which can be found in reference [23]. A circular yielding surface with isotropic hardening rule is chosen as our basic plastic model, so that it resembles the well-known J_2 associative plasticity theory for 2D analysis. It should be pointed out that no substantial difficulties are anticipated in incorporating other plastic models, if so desired. For the convenience of describing plastic flow, dimensionless stress and strain are used. The non-dimensional stress vector is defined as

$$s_1 = \frac{M}{M_0}, \quad s_2 = \frac{N}{N_0}, \quad \mathbf{s} = \{s_1 \quad s_2\}^T, \tag{50}$$

and the non-dimensional strain vector by

$$e_1 = \frac{M_0}{N_0}\kappa, \quad e_2 = \varepsilon, \quad \mathbf{e} = \{e_1 \quad e_2\}^T, \tag{51}$$

where M, N are the bending moment and axial force, and M_0, N_0 are the corresponding yield values under the single load condition. The elastic constitutive equation in terms of $\mathbf{s}$ and $\mathbf{e}$ is

$$\mathbf{s} = \mathbf{D}^* \mathbf{e}, \tag{52}$$

where

$$\mathbf{D}^* = \begin{bmatrix} EIn_0/m_0^2 & 0 \\ 0 & EA/n_0 \end{bmatrix}. \tag{53}$$

The yielding condition is formulated as

$$\phi(\mathbf{s}, \kappa) \equiv |\mathbf{s}| - s_0 - H\bar{e}^p = 0, \qquad \bar{e}^p = \int_0^t |\dot{\mathbf{e}}^p| \, \mathrm{d}\tau, \tag{54, 55}$$

where $|\mathbf{s}| = \sqrt{\mathbf{s}^T\mathbf{s}}$, the Euclidean norm $\bar{e}^p$ is the *equivalent plastic strain*, and serves as the plastic parameter $\mathbf{q}$ in section 3. The flow rule, in the form of non-dimensional plastic strain rate, is given by

$$\dot{\mathbf{e}}^p = \dot{\lambda}\frac{\partial \phi}{\partial \mathbf{s}}, \quad \dot{\bar{e}}^p = \dot{\lambda}. \tag{56}$$

Note that the plastic parameter λ and the yielding function ϕ satisfy the plastic loading and unloading condition (the Kuhn–Tucker condition). The elastoplastic constitutive equation is given as usual as

$$\dot{\mathbf{s}} = \mathbf{D}^*(\mathbf{e} - \dot{\lambda}\mathbf{n}). \tag{57}$$

The parameter $\dot{\lambda}$ can be eliminated by satisfying the plastic consistency condition. Performing the necessary algebraic manipulation [22], one gets the rate-form constitutive equation as

$$\dot{\mathbf{s}} = \mathbf{D}^*_{ep}\dot{\mathbf{e}}, \ \mathbf{D}^*_{ep} = \mathbf{D}^* - \gamma \mathbf{D}^*\mathbf{n}\mathbf{n}^T\mathbf{D}^*, \tag{58}$$

which in terms of the conventional stress and strain is

$$\mathbf{D}_{ep} = \mathbf{D} - \tilde{\gamma}\mathbf{D}\mathbf{n}'\mathbf{n}'^T\mathbf{D}, \tag{59}$$

where

$$\tilde{\gamma} = \gamma / n_0, \quad \mathbf{n}' = \mathbf{S}\mathbf{n}, \quad \mathbf{S} = \begin{bmatrix} n_0 / m_0 & \\ & 1 \end{bmatrix}. \tag{60}$$

Remark 3
Although both the bending moment and axial force appeared in the expression of tangential module matrix $\mathbf{D}_{ep}$, the transverse bending and axial tension will *not* be coupled unless geometric non-linearity is considered.

5.3. NUMERICAL EXAMPLE

A cantilever beam subjected to an impact load at its tip is used as an example to demonstrate the method. Its configuration, physical parameters and material properties are depicted in Figure 2. The spatial domain is evenly discretized into 20 elements. The quantities of interest are computed as follows: (1) the lowest natural frequency is $\omega_1 = 52\,\text{rad/s}$, (2) the longitudinal wave speed is $c = 2{\cdot}03(10^5)$ in/s.

To capture the propagation of the plastic zone, a time-step of $\Delta t = 4{\cdot}0 \times 10^{-5}\,\text{s}$ which satisfies $c \cdot \Delta t \approx \Delta L$, ΔL being the length of element employed, is adopted. For the purpose of comparison, the transient response at the tip of the beam predicted by STFEM for $\beta = 0{\cdot}25$ and $0{\cdot}50$, and by the Newmark method with ($\beta = 0{\cdot}25$, $\gamma = 0{\cdot}50$ are presented in Figure 3. As shown, the results deviate very little from each other.

The elastic and plastic responses are sketched in Figure 4. It is interesting to note that plastic deformations along the beam develop very rapidly, after which the whole beam unloads elastically with its period of oscillation almost unaltered; only its center of oscillation is shifted. This is perhaps characteristic of the elastoplastic behavior of structures under shock loading. The deformed configurations at various time-steps when plastic deformations are still evoluting and the corresponding elastic deformations are plotted in Figure 5. It can be seen that the propagation of shock waves is drastically slowed down by the

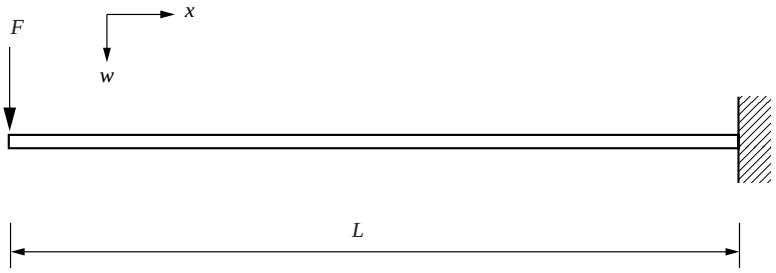

Figure 2. Cantilever beam subjected to an impact load: $E = 3{\cdot}0 \times 10^7$ psi, $G = 1{\cdot}2 \times 10^7$ psi, $I = 155{\cdot}3\,\text{in}^4$, $A = 44{\cdot}2\,\text{in}^2$, $L = 160\,\text{in}$, $\rho = 0{\cdot}773 \times 10^{-3}\,\text{lb s}^2/\text{in}^2$, $m_0 = 6{\cdot}33 \times 10^7\,\text{lb in}$, $H = 0{\cdot}1E$ and $F{\cdot}\Delta t = 100\,\text{lb s}$.

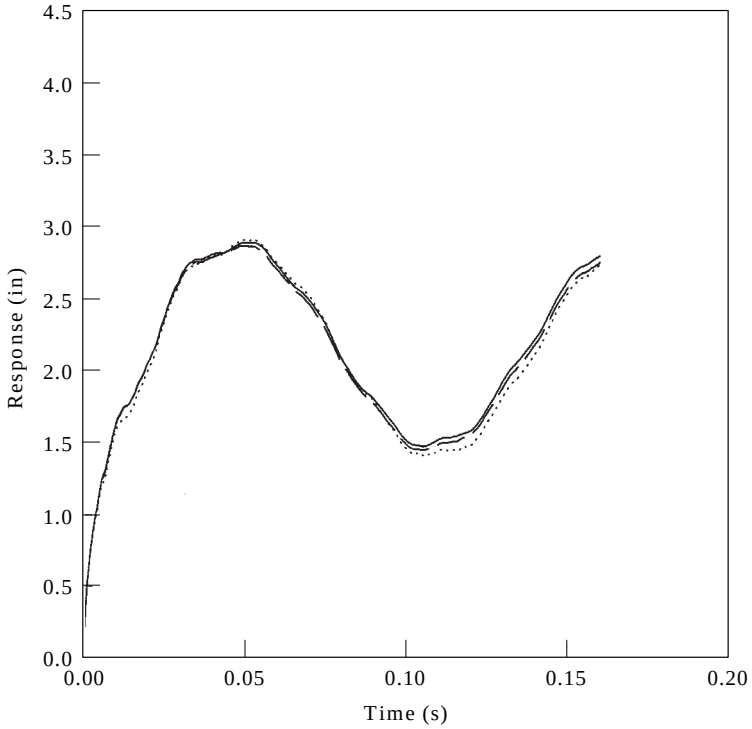

Figure 3. Comparison of tip response: ———, Newmark; — —, STFEM, $\beta = 0{\cdot}25$; ·····, STFEM, $\beta = 0{\cdot}50$.

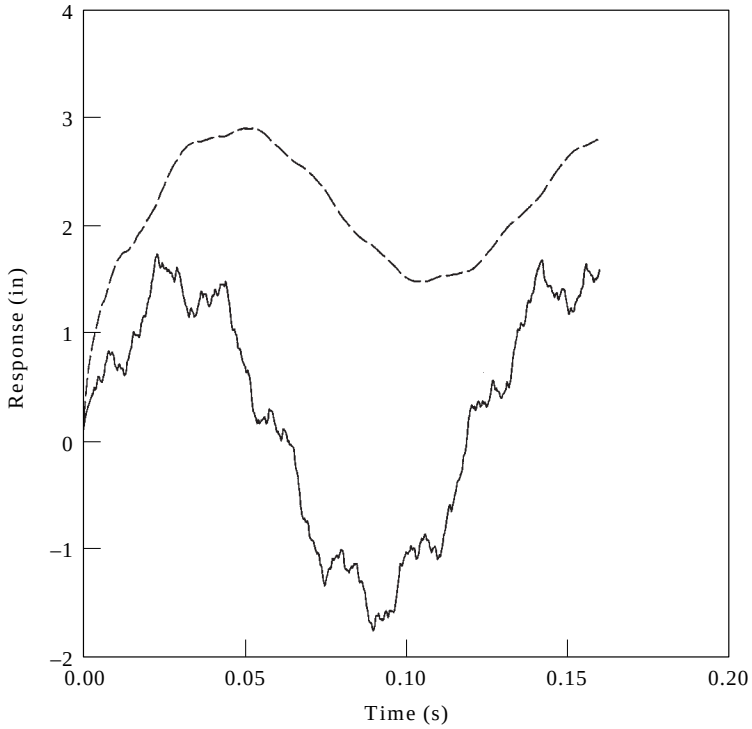

Figure 4. Elastic response versus plastic response; ————, linear elastic; — —, plastic.

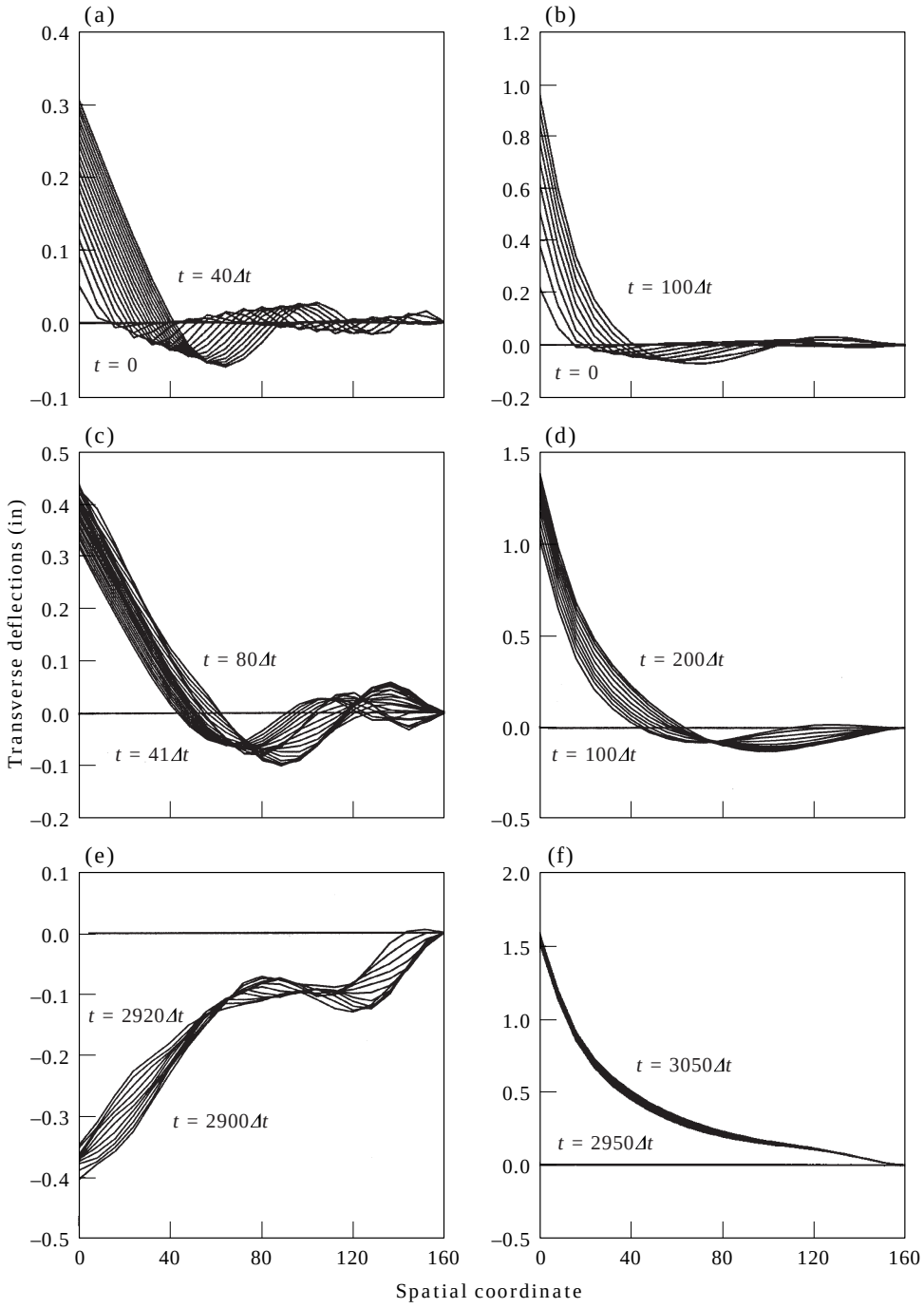

Figure 5. Deformed configurations: (a) $0 < t < 40\Delta t$, (b) $0 < t < 100\Delta t$, (c) $41\Delta t < t < 80\Delta t$, (d) $100\Delta t < t < 200\Delta t$, (e) $2900\Delta t < t < 2920\Delta t$, and (f) $2950\Delta t < t < 3050\Delta t$.

presence of plasticity. However, once the plastic deformations are fully developed, the wave speed recovers.

It would also be interesting to look at the evolution and distribution of plastic deformations. To this end the effective plastic strain along the length of the beam at various time-steps is plotted in Figure 6. Our first finding is that plastic deformations develop almost instantly, a matter that we have already pointed out. Also, plastic deformations tend to be localized in the vicinity of the point of impact which is expected. This implies that a full transient analysis is necessary for shock-dynamic problems, to accurately determine the location of the plastic hinges. For example, if a limit analysis were to be used for an assessment of this problem, a plastic hinge would be assumed to occur at the clamped end which is not the case at all. In fact, as the hardening parameter tends to zero, plastic deformations will become more localized, with the wave speed approaching zero. This of course, further reinforces our contention that a transient analysis is absolutely essential.

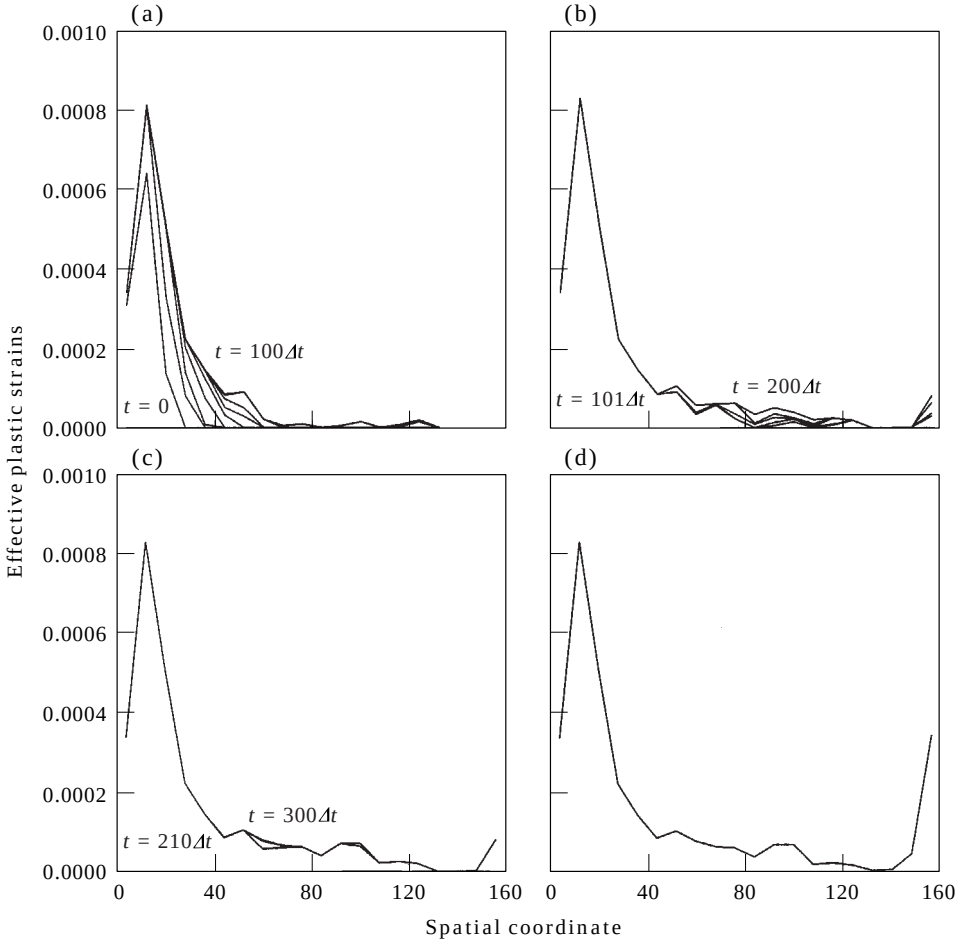

Figure 6. Propagation of the plastic zone; (a) $0 < t < 100\Delta t$, (b) $101\Delta t < t < 200\Delta t$, (c) $210\Delta t < t < 300\Delta t$, and (d) $2950\Delta t < t < 3050\Delta t$.

A comparison of the responses of damped and undamped systems is also provided. The purpose is to demonstrate the effectiveness of the present algorithm in handling damping forces. A Rayleigh damping of the form $\mathbf{C} = 20{\cdot}5\mathbf{M}$ is used. The resulting elastic response of both damped and undamped systems is presented in Figure 7 and the plastic counterpart in Figure 8. Obviously, the amplitude of the vibration is reduced by the presence of damping. Observe that the damping in general, will not affect the evolution and distribution of the plastic deformations significantly. Instead, it is the hardening parameter that plays this role, as mentioned previously.

6. CONCLUDING REMARKS

A STFEM scheme for elastoplastic dynamic analysis is proposed in this paper. A weak form of the governing equation which can be physically interpreted as the generalized *law of conservation of impulse-momentum* (the shock-momentum equation) is given. The space–time finite element is constructed by unifying conventional finite elements with piecewise linear time interpolations. Rate-independent plasticity is also incorporated into the model. It is found that the STFEM formulation is inherently suitable for handling the evolution equations of plastic flow. Also, the suggested STFEM formulation can actually lead to a rather broad range of algorithms, the one used to facilitate the computations here is just a special case, which for linear undamped elasticity, is equivalent to

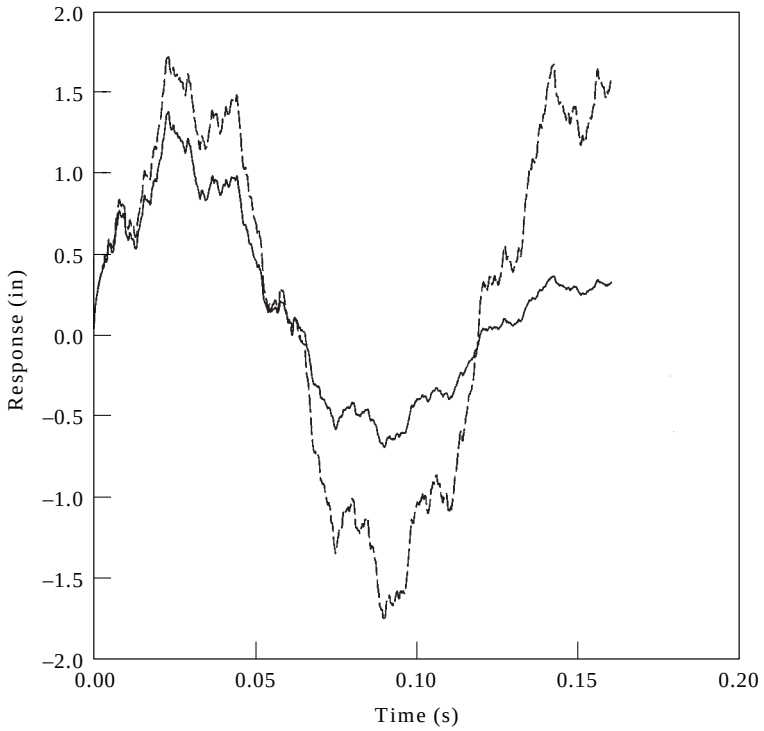

Figure 7. Elastic damped and undamped response: ————, damped; – – – –, undamped.

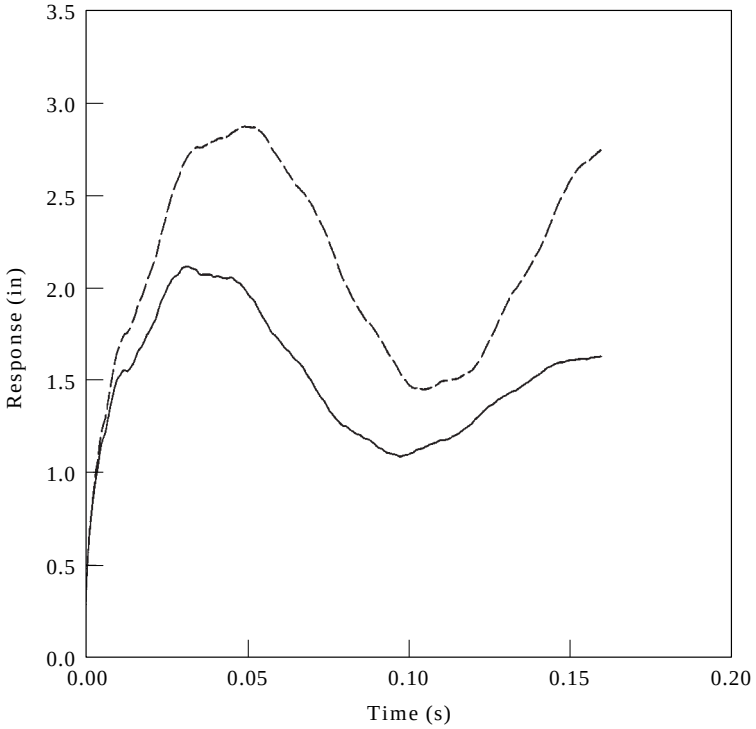

Figure 8. Plastic damped and undamped response: ————, damped; – – – –, undamped.

the Newmark method with $\gamma = 0{\cdot}5$. The status of current research is to focus on the use of discontinuous temporal interpolations for equation (14), and hopefully, this will lead to more accurate algorithms. The integration of evolution functions can also be cast in the STFEM formulation, and thus, a more uniformed framework for plastic transient analysis can be established. However, if the aim is to obtain an algorithm with symmetric consistent tangential operator, some more work needs to be done which is also being investigated. Finally, as demonstrated in the numerical simulations, plastic deformations develop almost instantly. They tend to be localized in the vicinity of the point of impact which implies that a full transient analysis is absolutely essential for structures subjected to shock loading. Also, it was shown that damping reduces the amplitude of the vibration, but will not, in general, affect the evolution and distribution of the plastic deformations significantly. Instead, it is the hardening parameter that plays this role.

ACKNOWLEDGMENT

In carrying out this research, financial support from the following source is gratefully acknowledged: Research Contract SSC XSG91-00142-(607) from Defense Research Establishment Suffield.

REFERENCES

1. O. C. Zienkiewicz 1991 *The Finite Element Method*, Volume 2. London: McGraw-Hill; fourth edition.
2. D. J. R. Owen and E. Hinton 1980 *Finite Elements in Plasticity*. Swansea: Pineridge Press Limited.
3. M. L. Wilkins 1964 in *Methods of Computational Physics*, Volume 3 (B. Alder, S. Fernback and M. Rottenberg, editors) 211—263. New York: Academic Press. Calculation of elastic-plastic flow.
4. R. D. Krieg and D. B. Krieg 1977 *Transactions of the American Society of Mechanical Engineers, Journal of Pressure Vessel Technology* **99**, 510–515. Accuracies of numerical solution methods for the elastic perfect plastic model.
5. J. Lubliner 1990 *Plasticity Theory*. New York: Macmillan Publishing Company.
6. K. Washizu 1982 *Variational Methods in Elasticity and Plasticity*. Oxford: Pergamon Press; third edition.
7. E. L. Wilson and R. E. Nickell 1966 *Nuclear Engineering and Design* **4**, 1–11. Application of finite element method to heat conduction analysis.
8. J. T. Oden 1969 *International Journal for Numerical Methods in Engineering* **l**, 247–259. A general theory of finite elements II. Applications.
9. J. H. Argyris and D. W. Scharpf 1969 *Nuclear Engineering and Design* **10**, 456–464. Finite elements in time and space.
10. I. Fried 1969 *American Institute of Aeronautics and Astronautics Journal* **7**, 1170–1173. Finite element analysis of time dependent phenomena.
11. O. C. Zienkiewicz 1977 *Earthquake Engineering and Structural Dynamics* **5**, 413–418. A new look at the Newmark, Houbolt and other time stepping formulas: a weight residual approach.
12. Li-min Tang, Ying-xi Liu and Zhen-feng Zhao 1990 *Acta Mechanica Solida Sinica* **3**, 201–208. A study of the finite element discretization technique in time domain.
13. P. Lesaint and P. A. Raviart 1974 in *Mathematical Aspects of Finite Element in Partial Differential Equations* (C. de Boor, editor) 89–123. New York: Academic Press. On a finite element method for solving the neutron transport equation.
14. P. Jamet 1978 *Society for Industrial and Applied Mathematics, Journal of Numerical Analysis* **15**, 912–928. Galerkin-type approximations which are discontinuous in time for parabolic equations in a variable domain.
15. C. Johnson 1987 *Numerical Solution of Partial Differential Equations by the Finite Element Method*. Cambridge: Cambridge University Press.
16. A. Cella, M. Lucchesi and G. Pasquinelli 1980 *International Journal for Numerical Methods in Engineering* **15**, 1475–1488. Space–Time finite elements for the shock wave propagation problem.
17. C. D. Bailey 1975 *Foundations of Physics* **5**, 433–451. A new look at Hamilton's principle.
18. M. Baruch and R. Riff 1982 *American Institute of Aeronautics and Astronautics Journal* **20**, 687–692. Hamilton's principle, Hamilton's law-6^n correct formulations.
19. R. P. S. Han and J. Lu 1995 *Final Report*, Contract SSC XSG91-00142-(607). Submitted to Defense Research Establishment, Suffield, Alberta. Development of a numerical method for nonlinear dynamic analysis of beams subjected to intense dynamic loads.
20. J. C. Simo and R. L. Taylor 1985 *Computational Methods in Applied Mechanics and Engineering* **48**, 101–118. Consistent tangent operators for rate-independent elasto-plasticity.
21. J. C. Simo, J. G. Kennedy and R. L. Taylor 1989 *Computational Methods in Applied Mechanics and Engineering* **89**, 177–206. Complementary mixed finite element formulations for elastoplasticity.

22. T. J. R. HUGHES and R. L. TAYLOR 1977 *International Journal for Numerical Methods in Engineering* **11**, 1529–1543. A simple and efficient finite element for bending.
23. R. P. S. HAN and J. LU 1993 *Progress Report* #7, Contract SSC X5G91-00142-(607). Submitted to Defense Research Establishment, Suffield, Alberta. An elasto-plastic beam element.